Cell Stem Cell
Article

Induction of a Human Pluripotent State with Distinct Regulatory Circuitry that Resembles Preimplantation Epiblast

Yun-Shen Chan,[1,6,*] Jonathan Göke,[1,6] Jia-Hui Ng,[1,6] Xinyi Lu,[1] Kevin Andrew Uy Gonzales,[1,2] Cheng-Peow Tan,[1] Wei-Quan Tng,[1,2] Zhong-Zhi Hong,[1] Yee-Siang Lim,[1] and Huck-Hui Ng[1,2,3,4,5,*]
[1]Gene Regulation Laboratory, Genome Institute of Singapore, Singapore 138672, Singapore
[2]Graduate School for Integrative Sciences and Engineering, National University of Singapore, Singapore 117456, Singapore
[3]Department of Biological Sciences, National University of Singapore, Singapore 117543, Singapore
[4]School of Biological Sciences, Nanyang Technological University, Singapore 637551, Singapore
[5]Department of Biochemistry, National University of Singapore, Singapore 117559, Singapore
[6]These authors contributed equally to this work.
*Correspondence: chanysw@gis.a-star.edu.sg (Y.-S.C.), nghh@gis.a-star.edu.sg (H.-H.N.)
http://dx.doi.org/10.1016/j.stem.2013.11.015

SUMMARY

Human embryonic stem cells (hESCs) are derived from the inner cell mass of the blastocyst. Despite sharing the common property of pluripotency, hESCs are notably distinct from epiblast cells of the preimplantation blastocyst. Here we use a combination of three small-molecule inhibitors to sustain hESCs in a LIF signaling-dependent hESC state (3iL hESCs) with elevated expression of *NANOG* and epiblast-enriched genes such as *KLF4*, *DPPA3*, and *TBX3*. Genome-wide transcriptome analysis confirms that the expression signature of 3iL hESCs shares similarities with native preimplantation epiblast cells. We also show that 3iL hESCs have a distinct epigenetic landscape, characterized by derepression of preimplantation epiblast genes. Using genome-wide binding profiles of NANOG and OCT4, we identify enhancers that contribute to rewiring of the regulatory circuitry. In summary, our study identifies a distinct hESC state with defined regulatory circuitry that will facilitate future analysis of human preimplantation embryogenesis and pluripotency.

INTRODUCTION

Embryonic stem cells (ESCs) are derived from the inner cell mass (ICM) of the blastocyst (Evans and Kaufman, 1981; Martin, 1981; Thomson et al., 1998) and are able to differentiate into the three germ layers and potentially into all cells of the adult body. This pluripotent property makes them invaluable in the field of regenerative medicine and as an important model for dissecting the biological processes of human embryonic development. Even though ESCs share the basic property of pluripotency with epiblast cells of the ICM, differences between the two have been observed (Nichols and Smith, 2012; Yan et al., 2013). A comparison of the expression profiles of human preimplantation blastocysts and hESCs highlighted that significant differences exist between pluripotency in vivo and in vitro (Reijo Pera et al., 2009; Vassena et al., 2011; Yan et al., 2013). In addition, signaling pathways such as the LIF/STAT3 pathway, which enhances blastocyst development (Dunglison et al., 1996), play no reported role in the self-renewal of hESCs (Dahéron et al., 2004; Humphrey et al., 2004). These differences are potentially established in the process of hESC isolation (Yan et al., 2013). Even though these differences are well recognized, no alternative hESC model systems have been described that more closely resemble cells of the native preimplantation epiblast.

Previous studies have reported that a number of cell types fulfill the criteria of pluripotency and that these distinct cells correspond to different embryonic developmental stages (Brons et al., 2007; Tesar et al., 2007). Interestingly, the different pluripotent cell states appear to be interconvertible. Conversion between these cell states has been achieved by the overexpression of the pluripotency associated transcription factors Nanog, Klf4, Nr5a2, and Stat3 (Silva et al., 2009; Guo et al., 2009; Guo and Smith, 2010; Yang et al., 2010), as well as the modulation of environmental signals provided by growth factors or perturbation of signaling pathways (Bao et al., 2009; Zhou et al., 2010). Factor-mediated conversion of different pluripotent states has also been successfully applied to human cells (Buecker et al., 2010; Hanna et al., 2010; Li et al., 2009; Wang et al., 2011), illustrating the feasibility of isolating distinct human pluripotent stem cell types. However, the requirement for the continual expression of these transgenes limits the potential for downstream application of these cells. Therefore, a transgene-free method for generating hESCs that more closely resemble the native pluripotent epiblast would be desirable. One approach to achieve this goal is the application of small molecules, which have been increasingly employed to manipulate cell fate in stem cells and can facilitate the isolation of cell states that are challenging for growth factor and cytokine-only culture conditions (Li et al., 2013; Zhang et al., 2012).

In this study, we use small molecules to target eight major signaling pathways to screen for culture conditions that can support a distinct human pluripotent stem cell state. We identify a combination of three small molecules that, together with LIF (3iL), support a distinct hESC state that more closely resembles the pluripotent epiblast cells of preimplanation blastocysts than

conventional hESCs. 3iL hESCs show increased expression of genes that are expressed in the epiblast such as *NANOG*, *DPPA3*, *KLF4*, and *TBX3*. We also find that the epigenetic landscape of 3iL hESCs indicates a global derepression of genes associated with pluripotent cells of human preimplantation embryos. To gain insights into how the transition toward the 3iL state occurs, we mapped the binding profile of OCT4, NANOG, and p300 by ChIP-Seq. This analysis highlighted numerous regulatory sites near epiblast-specific genes that are not detected in conventional hESCs, indicating the degree to which 3iL hESCs have the potential to model transcriptional regulation and epigenetics in early human embryogenesis.

RESULTS

A Combination of Small Molecules Induces a Unique hESC State

To induce an alternative hESC state that is potentially closer to the in vivo preimplantation epiblast state, we used 11 small molecules that target eight signaling pathways to screen for conditions that increase the expression of *NANOG* (Figure S1A available online). NANOG serves as a deterministic marker in the segregation of pluripotent epiblast from the hypoblast in the inner cell mass of preimplantation embryos (Kimber et al., 2008; Roode et al., 2012). The level of Nanog in mouse blastocyst is decreased during implantation (Chambers et al., 2003), suggesting that changing *Nanog* levels reflect different states of pluripotency. The expression of *NANOG* is also enriched in the human native preimplantation epiblast compared to hESCs (Yan et al., 2013). We first investigated the influence of these inhibitors individually. Although the cells treated with most of the small molecules stained positive for hESC markers, they did not exhibit a change in morphology or induce upregulation of the *NANOG* transcript (Figures S1B and S1C). We therefore proceeded to use combinations of these molecules (Figure S1D). In contrast to the usage of individual molecules, treatment with several combinations resulted in changes in both hESC morphology and upregulation of *NANOG* (Figure 1A, Figure S1E). In particular, combinations 21, 22, 23, and 24 induced a 1.5- to 2.0-fold increase in *NANOG* transcripts. *POU5F1* (*OCT4*) levels remained largely unchanged in these combinations (Figure 1A), suggesting that the cells are still pluripotent.

Next, we investigated whether chemical combinations 21 to 24 can stably sustain hESC self-renewal. However, we observed a strong impairment in proliferation for three of the conditions, such that few colonies survived after the first passage. Only hESCs treated with combination 22 (PD03/BIO/DOR, herein referred to as 3i) were able to form small, compact colonies on mouse fibroblast feeders (Figure 1B). However, the number of colonies decreased in each subsequent passage, indicating that self-renewal is disrupted (Figures 1C and 1D). As the morphology of these cells resembles that of mouse ESCs (mESCs), we investigated whether activation of signaling pathways that promote the self-renewal of mESCs can improve cell survival. LIF signaling is a key signaling pathway in the maintenance of mESCs (Niwa et al., 1998), the ICM (Do et al., 2013), and the conversion between mouse pluripotent states (Bao et al., 2009; Yang et al., 2010). Strikingly, addition of LIF could rescue the impaired self-renewal of 3i hESCs and enabled these cells to be stably propagated for more than 30 passages (Figures 1C and 1D). These 3i+LIF-treated hESCs (herein referred to as 3iL hESCs) form smaller and more compact colonies than hESCs cultured in TeSR1 media (herein referred to hESCs) (Figure 1E). In contrast to hESCs, 3iL hESCs can survive the passage as single cells without the addition of ROCK inhibitor (Figure 1F). The combinatorial use of the three inhibitors is important to maintain the 3iL hESC state as the cells cannot be maintained when individual chemicals are removed from the media (Figure S1G). In summary, the application of three inhibitors and LIF enables the efficient propagation of hESCs that are distinct from conventional hESCs.

Active LIF signaling in 3iL hESCs

In contrast to conventional hESCs, which do not depend on LIF signaling (Dahéron et al., 2004; Humphrey et al., 2004), LIF appears to be essential for the self-renewal of 3iL hESCs. To further investigate the role of LIF in 3iL hESCs, we used a Jak inhibitor (inh) that targets the LIF signaling pathway (Hanna et al., 2010; Yang et al., 2010). Treatment of 3iL hESCs with the Jak inh induced a decrease in pluripotency marker expression and a strong reduction in colony numbers (Figures 2A and 2B). Gene expression of *NANOG* and LIF signaling-responsive genes *KLF4* and *SOCS* was reduced (Figure 2C). These results further indicate that LIF signaling is required for the maintenance of 3iL hESCs.

LIF signaling can be induced in hESCs (Dahéron et al., 2004). However, in contrast to 3iL hESCs, LIF is not essential for hESC self-renewal. To investigate the cause of the difference in LIF requirement, we compared LIF signaling activity in both cell states. In hESCs, the transcript of *GP130*, which is the coreceptor essential for LIF activity (Ip et al., 1992), is poorly expressed relative to other components of the LIF signaling pathway (Figure 2D). A short treatment of hESCs with 3i and stable culture of hESCs in 3iL both resulted in upregulation of *GP130* transcript (Figures 2E and 2F) and protein levels (Figure 2G), indicating that these cells have become more sensitive to LIF signaling. Correspondingly, the level of phosphorylated STAT3 was also significantly higher in 3iL hESCs compared to hESCs that were cultured with LIF alone (Figure 2H), suggesting that LIF signaling is more active in 3iL hESCs. The expression levels of known STAT3 targets *SOCS3* and *KLF4* were also increased in hESCs treated with 3i+LIF compared to LIF alone (Figure 2I). Interestingly, *NANOG* expression levels increased with the addition of LIF in a dosage-dependent manner under 3i treatment, suggesting that *NANOG* might be a direct target of LIF signaling (Figure S2A). These results indicate that while 3i treatment could not sustain hESC self-renewal, it induces a hESC state that is highly responsive to LIF signaling. In this scenario, elevated LIF signaling becomes essential for maintenance of the pluripotent cell state.

We next investigated whether other signaling pathways important in hESCs also play a role in 3iL hESCs. The FGF, PI3K, and Activin signaling pathways have been reported to be important for the maintenance of hESCs (Göke et al., 2013; Singh et al., 2012; Vallier et al., 2005). We treated 3iL hESCs with the respective small-molecule inhibitors of these three signaling pathways and also of EGF signaling, which does not have a described role in hESCs, as a negative control. The inhibition of FGF, PI3K, and Activin signaling pathways resulted in the loss of pluripotency markers after 10 days of treatment (Figures S2B

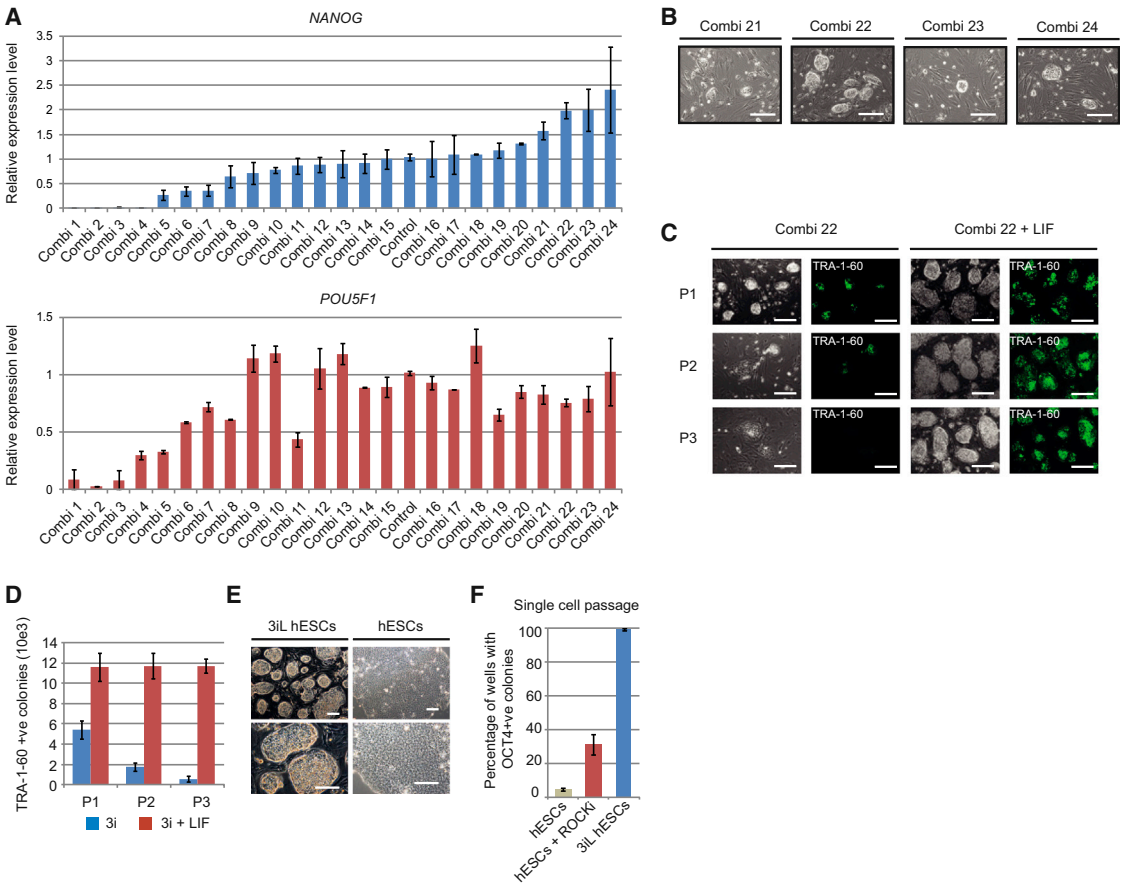

Figure 1. Small-Molecule Treatment of hESCs Induces a Novel LIF-Dependent hESC State

(A) Expression levels of pluripotency markers *NANOG* (top) and *POU5F1* (bottom) for hESCs that were treated for 4 days with 24 different combinations of small molecules 48 hr postseeding. Relative expression is obtained via normalization against the control samples treated with DMSO. All values are mean ± SD from three independent experiments.

(B) Propagation of hESCs treated with chemical combinations 21 to 24 on mouse fibroblast feeders. Only hESCs treated with combination 22 form small compact colonies. Scale bar represents 200 μm.

(C) Cells treated with combination 22 proliferate only in the presence of human LIF. Cells treated with combination 22 were continuously subcultured with or without LIF. For each passage (P1–P3), cells were fixed upon confluency and stained with hESC-specific surface marker TRA-1-60. Scale bar represents 200 μm.

(D) Shown are the numbers of TRA-1-60 positive colonies for hESCs cultured in 3i, with or without LIF (P1-3). All values are mean ± SD from three independent experiments.

(E) Morphology of 3iL hESCs and hESCs. Scale bar represents 200 μm.

(F) 3iL hESCs can be subcultured as single cells. 3iL hESCs and hESCs were subcultured as single cells into 96-well culture dishes at clonal density. hESCs treated with and without ROCK inhibitor (1 μM Thiazovivin) served as control. The cells were maintained for 5 days, fixed, and stained for OCT4. All values are mean ± SD from three independent experiments.

See also Figure S1.

and S2C). This result suggests that other signaling pathways are still required to act in conjunction with the LIF signaling pathway to support the unique 3iL hESC state.

3iL hESCs Exhibit Hallmarks of Pluripotency

We next proceeded to characterize whether these 3iL hESCs are indeed pluripotent. The cells stained positive for pluripotency markers OCT4, NANOG, TRA-1-60, and TRA-1-81 (Figure 3A). The transcript levels of the pluripotency markers remained comparable between 3iL hESCs and untreated hESCs (Figure 3B). 3iL hESCs maintained a 2-fold higher level of *NANOG* expression (Figure 3B), which was also reflected at the protein level (Figure 3C). Interestingly, we observed an upregulation of epiblast-enriched genes (Reijo Pera et al., 2009; Vassena et al., 2011; Yan et al., 2013) including *DPPA3*, *KLF4*, and *TBX3* in 3iL hESCs (Figure 3B). FACS analysis reveals that 3iL hESCs clearly expressed OCT4 and have a marked increase in NANOG, TRA-1-60, and TRA-1-81 levels (Figure 3D).

Next, we investigated whether the 3iL hESCs could differentiate into all germ lineages. 3iL hESCs form large embryoid bodies that can differentiate to cells of the extraembryonic lineage and all three germ layers (Figure 3E). In vivo, 3iL hESCs also generated tissues of all three germ layers when injected into immunodeficient mice (Figure 3F). Interestingly, the 3iL hESCs generated teratomas of a larger volume in a shorter time than hESCs (Figure 3G). Importantly, 3iL hESCs maintained a normal karyotype

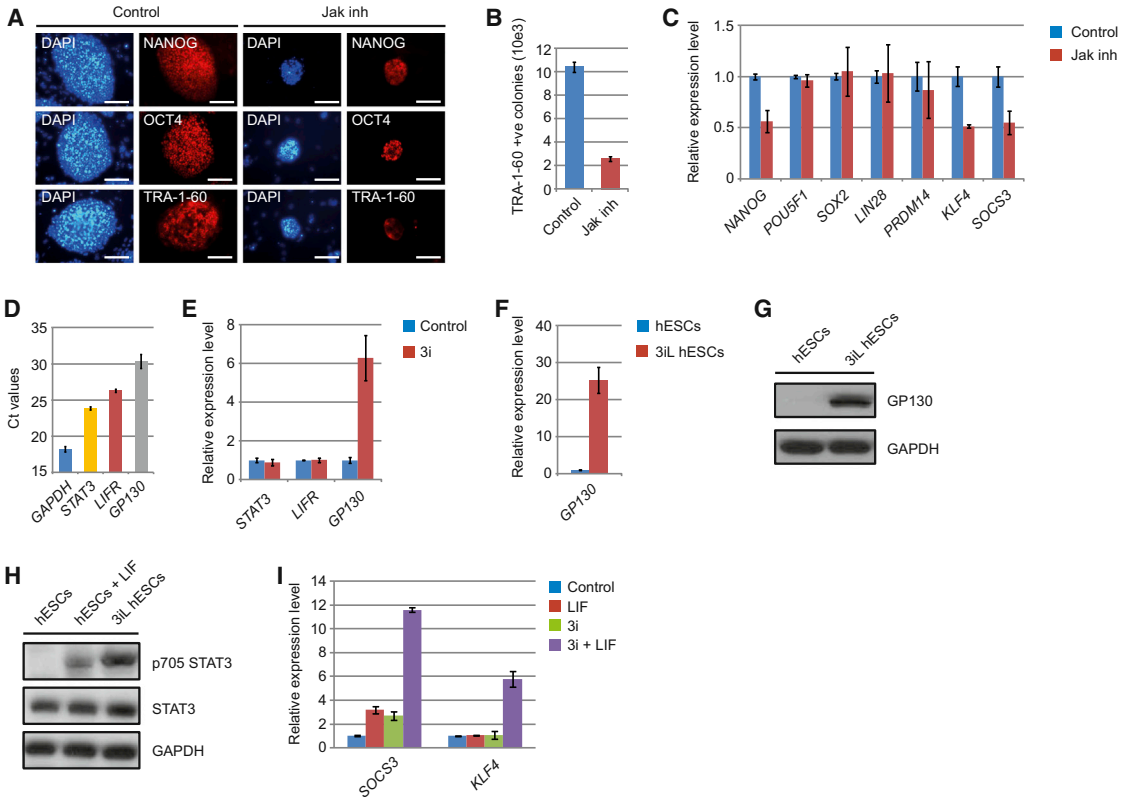

Figure 2. Self-Renewal of 3iL hESCs Is Dependent on LIF Signaling

(A) 3iL hESCs were treated with 0.6 μM of Jak inhibitor (inh). Control cells were treated with DMSO. The cells were fixed after 10 days of treatment and stained for pluripotency markers NANOG, OCT4, and TRA-1-60.

(B) Number of TRA-1-60-positive colonies in 3iL hESCs with and without Jak inh. All values are means ± SD from three independent experiments.

(C) Expression of pluripotency genes and LIF signaling responsive genes in hESCs with and without Jak inh. All values are mean ± SD from three independent experiments.

(D) Expression of LIF signaling components in hESCs. Shown are the average Ct values of *STAT3*, *LIFR*, *GP130*, and housekeeping gene *GAPDH*. The high Ct value indicates that *GP130* is poorly expressed in hESCs. All values are mean ± SD from three independent experiments.

(E) Induction of *GP130* expression when hESCs were treated with 3i. Relative expression levels were obtained via normalization against a control sample treated with DMSO. All values are mean ± SD from three independent experiments.

(F) Relative expression level of *GP130* in 3iL hESCs and hESCs. All values are mean ± SD from three independent experiments.

(G) Upregulation of GP130 protein in 3iL hESCs compared to hESCs. Antibody specific to GP130 was used to detect the presence of GP130 in whole cell extract of 3iL hESCs and hESCs.

(H) 3iL hESCs show higher levels of phosphorylated STAT3 compared to LIF-treated hESCs. Whole-cell extracts of hESCs, hESCs cultured with 10 ng/ml of LIF, and 3iL hESCs were used to determine the level of STAT3 phosphorylation in the respective culture condition. The GAPDH protein level served as a loading control. Addition of LIF weakly activates STAT3 phosphorylation compared to the 3iL culture condition.

(I) Activation of STAT3 responsive genes *SOCS3* and *KLF4* in hESCs after treatment with 3i, 3iL, or LIF for 4 days. All values are mean ± SD from three independent experiments.

See also Figure S2.

after 2 months of culture in the 3iL condition (Figure 3H). These results show that 3iL hESCs are indeed pluripotent. To confirm that the 3iL hESC state is not unique to H1 hESC, we tested the 3i+LIF small-molecule combination on two other human hESC lines, hES2 and hES3 (Figures S3A–S3L). We observed reproducible changes in morphology, induction of marker expression, and the ability to differentiate to all three germ layers in teratomas. As both our TeSR1-cultured hES2 and hES3 hESCs showed erosion of X inactivation, we were unable to examine the X-reactivation in the 3iL culture condition. We next tested whether the 3iL condition enables maintenance of human induced pluripotent stem cells (iPSCs). We treated reprogrammed cells with 3iL conditions after 3 weeks of virus induction. While we did not observe an increase in total number of iPSC colonies (Figure S3M), we observed a significant improvement in virus silencing in the colonies that did emerge (Figures S3N and S3O), suggesting an increase in the number of bona fide iPSC colonies (Chan et al., 2009). iPSC clones can also be stably cultured in 3iL conditions (Figures S3P–S3R). These data confirm that the induction of a distinct cell state by 3iL can be achieved across different human pluripotent cell types.

The Transcriptome of 3iL hESCs Resembles Native Preimplantation Epiblast

The above results indicate that 3iL hESCs are distinct from hESCs. To characterize these differences, we compared the

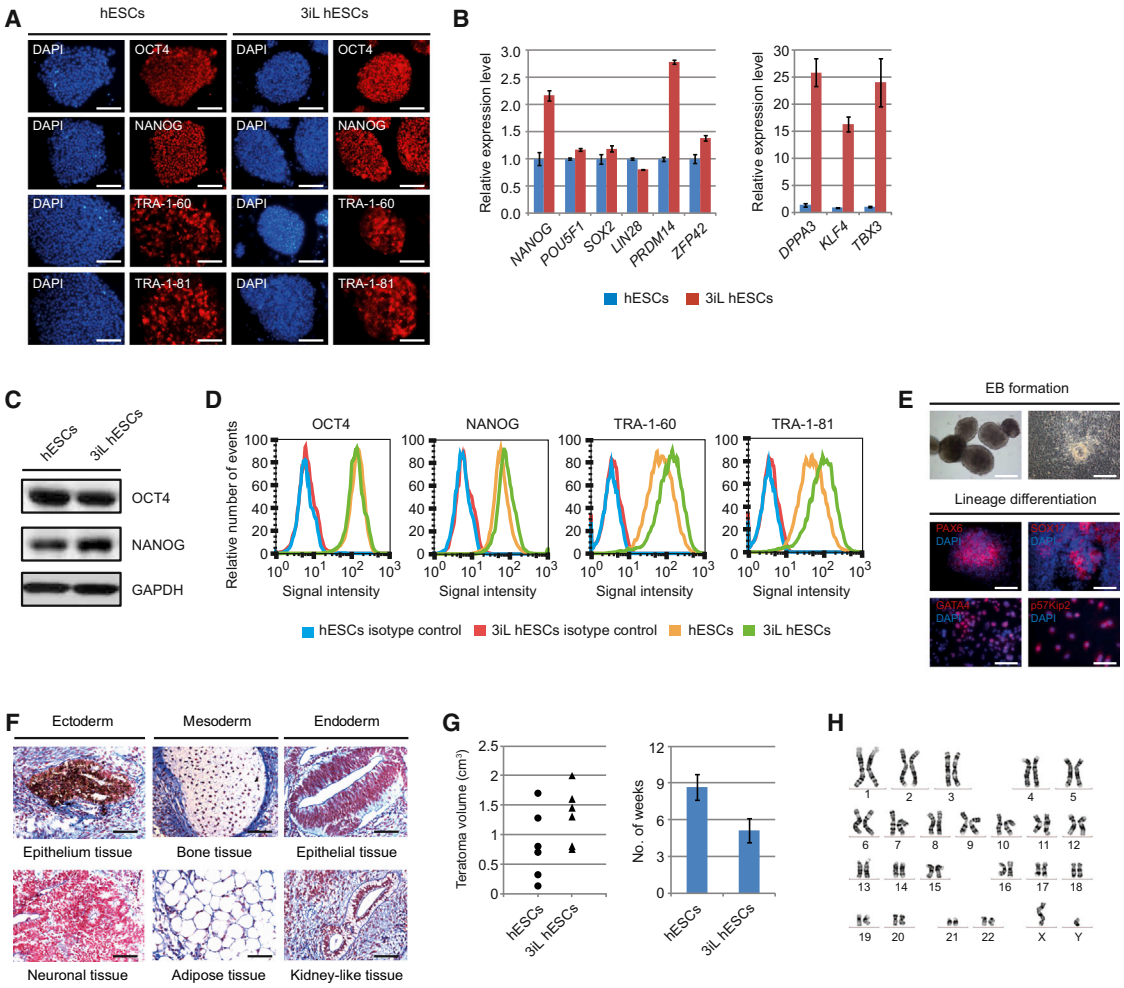

Figure 3. 3iL hESCs Are Pluripotent

(A) Staining of 3iL hESCs and hESCs for pluripotency markers NANOG and OCT4, and hESCs-specific cell-surface markers TRA-1-60 and TRA-1-81. Scale bar represents 200 μm.

(B) Relative expression of pluripotency-associated genes and epiblast genes in hESCs and 3iL hESCs. All values are mean ± SD from three independent experiments.

(C) Western blot analysis of protein levels for NANOG and OCT4 in hESCs and 3iL hESCs. Corresponding to the increase in *NANOG* gene expression level, the NANOG protein level in 3iL hESCs is higher compared to hESCs.

(D) FACS analysis of pluripotency markers in 3iL hESCs and hESCs indicates that 3iL hESCs express higher levels of NANOG, TRA-1-60, and TRA-1-81.

(E) 3iL hESCs form embryoid bodies (EBs) in suspension culture and differentiate into the three germ layers and trophectoderm in vitro. Shown are 3iL hESC-derived EBs cultured for 20 days in suspension (top left panel) and the adhesion and expansion of embryoid bodies plated onto gelatin plates (top right panel). 3iL hESCs can differentiate into ectoderm (PAX6), definitive endoderm (SOX17), mesoderm (GATA4), and trophectoderm (p57Kip2). Scale bar represents 200 μm.

(F) 3iL hESCs form teratomas when injected into SCID mice. Shown are teratoma sections containing tissues that are representative of all three embryonic germ layers. Scale bar represents 50 μm.

(G) 3iL hESCs form teratomas more efficiently than hESCs. Volume of teratoma formed by 3iL hESCs (left panel) and average time taken for the formation of the teratoma (right panel). Shown are six replicates for each condition.

(H) 3iL hESCs exhibit a normal karyotype after 2 months in culture.

See also Figure S3.

transcriptome of 3iL hESCs and hESCs using RNA-Seq. First we identified genes that showed significant changes in expression levels between 3iL hESCs and hESCs, further referred to as 3iL hESC-specific (increased expression in 3iL hESCs) and hESC-specific genes (decreased expression 3iL hESCs) (Table S1). The 3iL-specific genes included *NANOG*, *DPPA3*, *KLF4*, and *TBX3* (Figure 4A), confirming our initial observations. To investigate whether 3iL hESCs resemble in vivo pluripotent cells, we compared the 3iL hESC expression data with single-cell RNA-Seq data from human preimplantation embryos and primary hESCs derived from blastocysts at passage 0 and 10 (Yan et al., 2013). Strikingly, we found that 3iL hESC-specific genes show significantly higher expression in preimplantation blastocyst cells than hESC-specific genes (Figure 4B). In contrast, hESC-specific genes show higher expression than 3iL hESC-specific genes in primary hESC outgrowths from the blastocyst

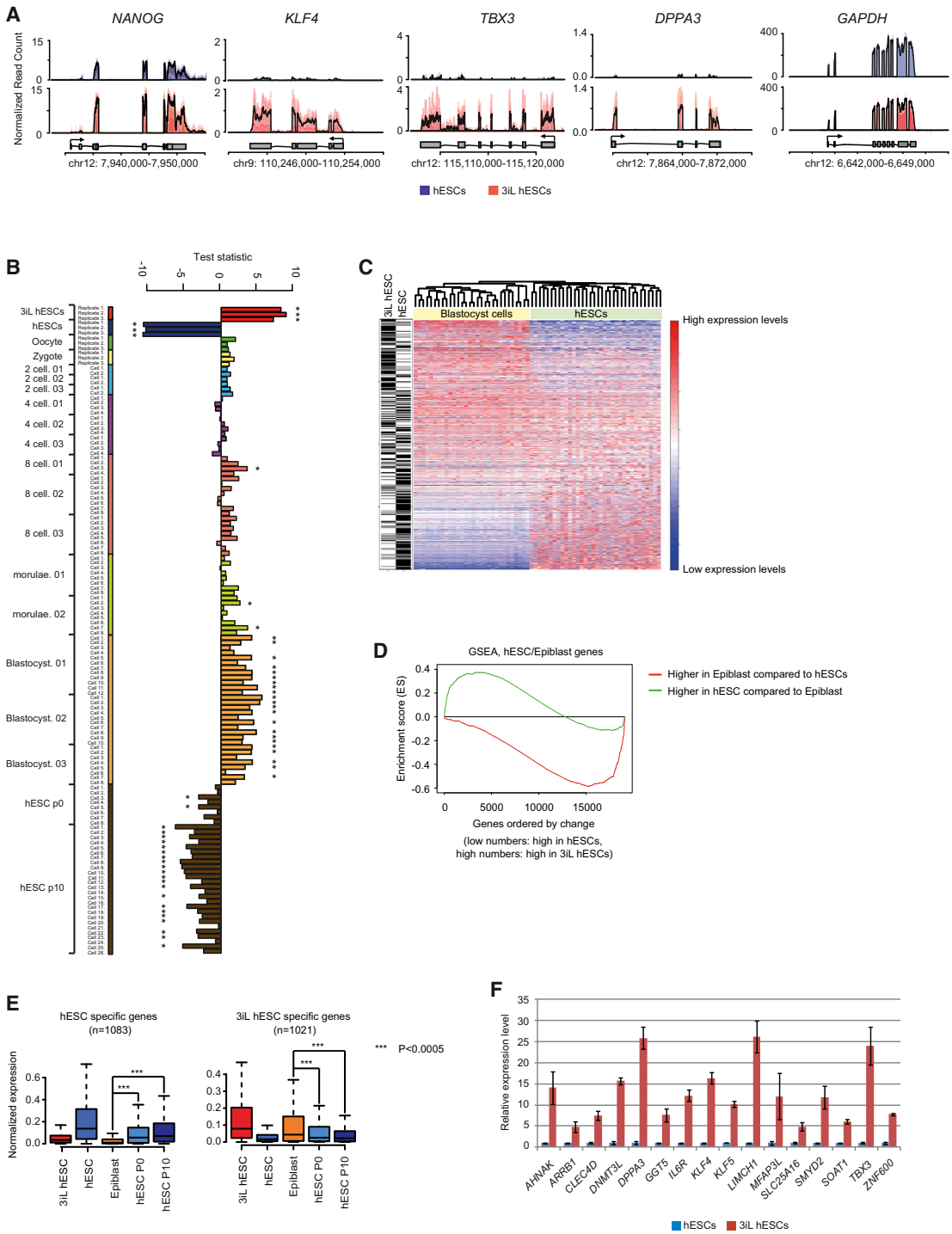

Figure 4. The Transcriptome of 3iL hESCs Resembles In Vivo Preimplantation Epiblast

(A) The normalized RNA-Seq read count of *NANOG*, *KLF4*, *TBX3*, *DPPA3*, and *GAPDH* in hESCs (blue) and 3iL hESCs (red). The black line shows the mean of three replicates; the individual replicates are shown in light-blue and light-red, respectively (overlayed). Read counts were normalized by the number of mapped reads for every replicate. Coordinates are for human genome version hg19.

(B) Comparison of expression of 3iL-specific genes with expression of hESC-specific genes in preimplantation embryos. Shown is the test statistic from an unpaired t test; positive values indicate that 3iL-specific genes show higher expression than hESC-specific genes and vice versa for negative values. Significant differences (multiple testing adjusted p value < 0.05) are marked with *. The data were normalized per sample and gene prior to testing.

(C) Heatmap showing single-cell gene expression from preimplantation blastocyst and hESCs for genes that are differentially expressed between 3iL hESCs and hESCs. Clustering was done on this set of genes using hierarchical clustering. Genes are sorted by the fold change of average expression between blastocyst and hESCs. Differentially expressed genes (3iL hESCs versus hESCs) are marked by black lines.

(legend continued on next page)

(Figure 4B). Importantly, the set of 3iL hESC-specific and hESC-specific genes is sufficient to discriminate hESCs from preimplantation blastocyst cells based on single-cell RNA-Seq data (Figure 4C). The ICM of the profiled blastocyst (Yan et al., 2013) consists of cells of the pluripotent epiblast (EPI) and cells of the primitive endoderm (PE) (Roode et al., 2012). As we were particularly interested in the epiblast cells of the blastocyst, we assessed the expression of putative EPI-specific genes (Yan et al., 2013) in 3iL hESCs. Genes that are expressed at a higher level in EPI cells compared to hESCs (epiblast-specific genes) are significantly enriched in 3iL hESCs (Figures 4D and 4E, Figures S4A–S4D). Increased expression of these epiblast-specific genes in 3iL hESCs is further confirmed by quantitative PCR (Figure 4F). Single-cell PCR data confirm that pluripotency genes and epiblast genes are indeed coexpressed and not a result of a heterogeneous cell population (Figure S4E). Thus, 3iL treatment induces conversion of hESCs toward a cellular state that more closely resembles pluripotent cells from the human preimplantation embryo.

Coexpression of GATA6 and NANOG in 3iL hESCs

One of the genes that is expressed in blastocyst (Yan et al., 2013) and 3iL hESCs but not in conventional hESCs is GATA6 (Figure S4F). GATA6 has been reported to be able to replace OCT4 during reprogramming (Shu et al., 2013) and is expressed in early preimplantation embryos (Guo et al., 2010; Kimber et al., 2008; Roode et al., 2012). As GATA6 is also implicated in primitive endoderm (Kuijk et al., 2012) and mesoderm differentiation (Abe et al., 2003), we wanted to exclude the possibility that GATA6 expression is caused by spontaneous differentiation. Examination of the expression of pluripotency-associated genes indicated that these genes show similar expression levels in 3iL hESCs and hESCs (Figure S4G). Validation by quantitative PCR also confirms that differentiation-associated genes are not upregulated in 3iL hESCs (Figure S4H). We further confirmed the expression of *GATA6* in the 3iL hESCs with quantitative PCR and the protein levels with western blot analysis (Figures S4I and S4J). Coimmunostaining of GATA6 and NANOG reveals the coexpression of these two proteins in 3iL hESCs (Figure S4K). To further confirm this result, we performed flow cytometry analysis and found that, remarkably, more than 50% of the 3iL hESCs express both NANOG and GATA6 compared to less than 5% in the hESCs (Figure S4L). GATA6 is also coexpressed with OCT4 and TRA-1-60 (Figures S4M and S4N). These results indicate that expression of *GATA6* is not caused by differentiation or loss of pluripotency, but rather reflects a specific property of 3iL hESCs. NANOG and GATA6 are coexpressed in cells within the ICM of the blastocyst before the segregation of the pluripotent epiblast from the hypoblast (Roode et al., 2012). Our results suggest that 3iL hESCs resemble these NANOG and GATA6 coexpressing cells. As such, 3iL hESCs could provide a model to study the role of GATA6 and other early embryonic developmental genes in pluripotency (Plusa et al., 2008; Roode et al., 2012).

Derepression of Preimplantation Epiblast-Associated Genes in 3iL hESCs

To investigate whether the gene expression profile of 3iL hESCs is stabilized by a concomitant change in the epigenetic landscape, we generated genome-wide profiles of histone modifications associated with active (H3K27ac, H3K4me3) and repressive (H3K27me3) chromatin. For every gene, we calculated a normalized fold change of the respective histone marks between 3iL hESCs and hESCs. Indeed, we find that the change in gene expression is accompanied by a global change in histone modifications at relevant promoters (Figures 5A and 5B). Genes that show increased expression in 3iL hESCs are significantly enriched in the set of genes that show an increase of active histone modifications H3K27ac (p value = 8.83e-263) and H3K4me3 (p value = 2.38e-69), and a reduction in H3K27me3 (p value = 4.90e-92), which is a repressive mark usually associated with developmental genes (Figure 5B). Strikingly, when we investigated promoters of genes which are differentially expressed in the native preimplantation epiblast and in vitro hESCs, we found that loss of H3K27me3 occurs at epiblast-specific genes (Figure 5C). Thus, genes such as *TBX3*, *KLF5*, *ZNF600*, and *HOXB* cluster that are silenced during derivation of hESCs from the blastocyst show reactivation in 3iL hESCs (Figure 5D, Figure S5). Together these data indicate that 3iL hESCs reside in a distinct state that provides a unique model for studying the epigenetics of preimplantation embryogenesis.

A Rewired Regulatory Circuitry in 3iL hESCs

The gene regulatory network that controls pluripotency has been studied in ESCs (Boyer et al., 2005; Chen et al., 2008) and has provided fundamental insights into the regulation of embryonic stem cell identity. Our analyses of gene expression and epigenetic modifications suggest that 3iL hESCs represent a pluripotent state that is distinct from conventional hESCs. To investigate whether the transcriptional regulatory network is different in the two cell states, we generated genome-wide binding maps of the master pluripotency regulators NANOG and OCT4, as well as the general enhancer binding protein P300. For every binding site of OCT4, NANOG, and P300, we examined differential binding between 3iL hESCs and conventional hESCs to identify 3iL-specific and hESC-specific binding events. Strikingly, we find that thousands of binding events change between the two pluripotent states, indicating that the regulatory

(D) Gene Set Enrichment Analysis (GSEA). Genes were ranked according to the fold change in expression between 3iL hESCs and hESCs. Shown is the enrichment for genes which are differentially expressed in hESCs and human epiblast (Yan et al., 2013). Genes that show increased expression in 3iL hESCs are enriched in the set of epiblast-specific genes (red line, Wilcoxon rank-sum test p value = 1.03e-48), whereas genes that show increased expression in conventional hESCs are enriched in the set of genes that show higher expression in hESCs compared to human epiblast (green line, p value = 1.61e-20).
(E) Normalized expression of hESC-specific genes and 3iL hESC-specific genes in 3iL hESCs, hESCs, human preimplantation epiblast (average from single cell data), hESCs passage 0 (average from single cell data), and hESCs passage 10 (average from single cell data). p values were calculated using a paired t test. The number of genes corresponds to genes that are differentially expressed in 3iL hESCs and hESCs and where expression is provided by (Yan et al., 2013).
(F) Real-time qPCR validation of epiblast-specific genes that are upregulated in 3iL hESCs compared to hESCs. All values are mean ± SD from three independent experiments.
See also Figure S4 and Table S1.

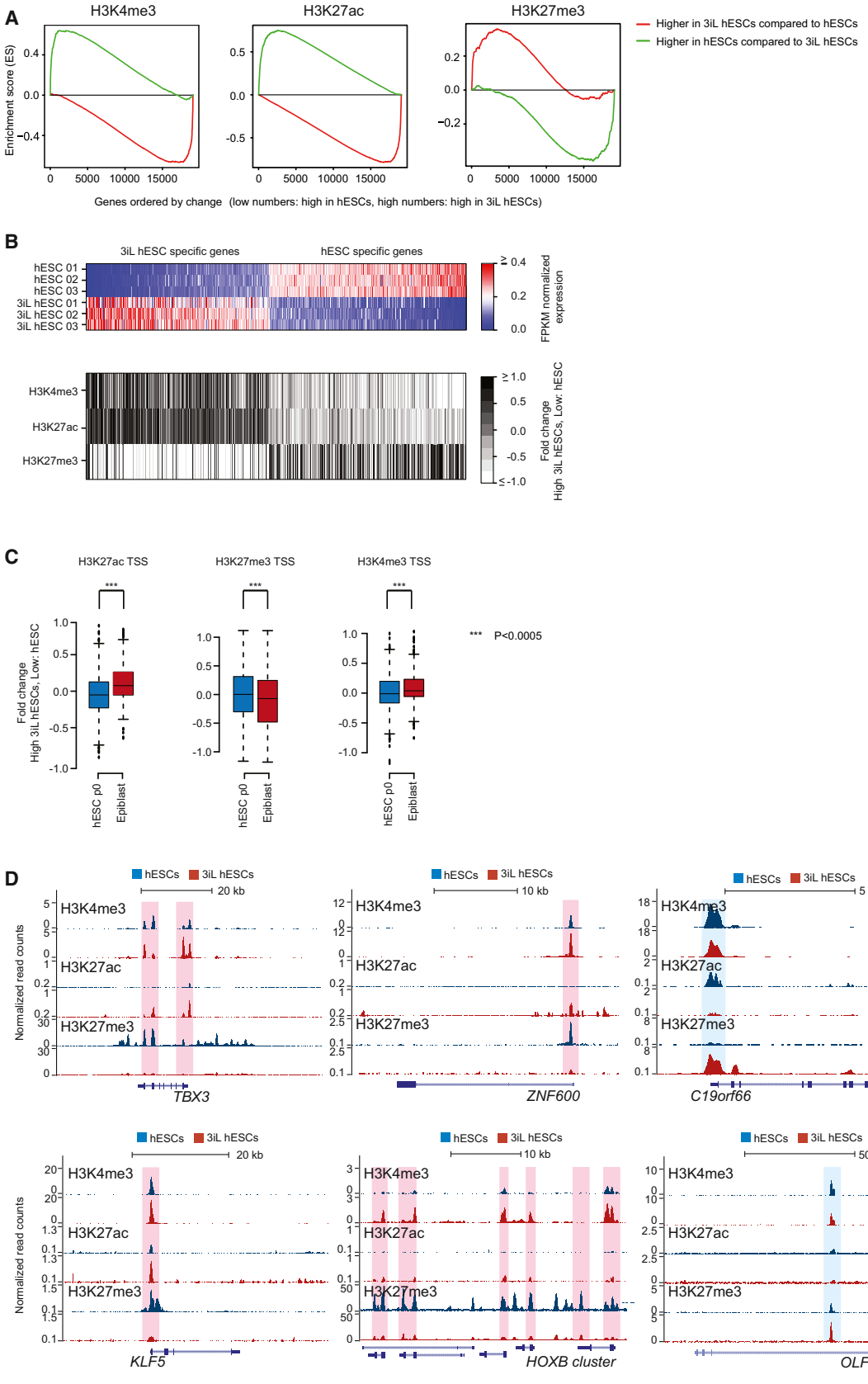

(legend on next page)

network indeed is rewired (Table S2, Table S3, Figure S6A). In support of a rewired network, we find that transcription factor differential binding is significantly associated with differential expression of their target genes (Figure 6A).

As 3iL hESCs show epigenetic and transcriptional reactivation of epiblast-specific genes that are silenced in conventional hESCs, we investigated whether 3iL hESCs can be used to identify enhancers that may be active in human preimplantation development. We found that the increase in NANOG occupancy at distal enhancers is significantly associated with upregulation of epiblast-specific genes (Figure 6B) (Fisher's test p value = 5.46e-13, Table S4). The genes that are expressed in the native preimplantation epiblast and that show new or enhanced binding sites in 3iL hESCs include *NANOG*, *KLF4*, *DPPA3*, *KLF5*, *DNMT3L*, *TBX3*, *ZNF600*, and *LAMB1* (Figures 6B and 6C, Figure S6B). Interestingly, we also detected STAT3 binding near some of these genes (Table S5), suggesting that LIF signaling may integrate with the core pluripotency network in 3iL cells (Figures 6B and 6C).

DISCUSSION

In this study, we show that combinatorial treatment with three small molecules successfully induces a distinct hESC state that is different from conventionally cultured hESCs. These 3iL hESCs require LIF to self-renew, and share an expression signature with pluripotent epiblast cells of the native human blastocyst. Single-cell analysis of human preimplantation embryos and hESCs has revealed significant differences between the two (Yan et al., 2013). The 3iL hESC state that we have characterized here narrows the gap between these in vivo and in vitro pluripotent states (Figure 6D). The simlarity between 3iL hESCs and native preimplantation epiblast cells provides a platform for future studies in deciphering the molecular pathways that specify pluripotency.

hESCs have been maintained in multiple chemically defined conditions (Furue et al., 2008; Lu et al., 2006; Ludwig et al., 2006; Vallier et al., 2005; Yao et al., 2006) using various external signaling factors, including LIF (Gafni et al., 2013). The recently reported LIF-dependent hESCs appear to be similar to naive mESCs (Gafni et al., 2013). Through a different screening strategy, we identified a distinct LIF-dependent pluripotent state that harbors a native preimplantation epiblast gene expression signature. Further work needs to be carried out to compare the molecular and functional properties of naive hESC, 3iL hESC, and in vivo pluripotent states. We observed STAT3 binding sites in the 3iL hESC transcriptional regulatory circuitry, suggesting that LIF signaling may contribute to the 3iL hESC expression signature. LIF signaling has been reported to enhance the formation of human blastocysts in vitro (Dunglison et al., 1996). However, how LIF signaling could play a role in pluripotent cells of the blastocyst remains unknown. Hence, dissecting the role of LIF in 3iL hESCs could provide a better understanding of how LIF signaling contributes to blastocyst development.

One of the hallmarks of 3iL hESCs is upregulation of a group of genes that are expressed in early human embryogenesis, some of which are thought to act as lineage specifiers. An example is GATA6, which is expressed in the early ICM of both mouse and human embryos (Guo et al., 2010; Roode et al., 2012). Interestingly, GATA3, GATA4, and GATA6 were able to replace OCT4 in reprogramming (Montserrat et al., 2013; Shu et al., 2013), indicating a role of lineage specifiers in induced pluripotency. Although the *GATA6* locus is bound by OCT4, NANOG, and STAT3, the role of GATA6 in the 3iL hESCs remains to be elucidated. In the 3iL hESCs, GATA6 could be a component of the pluripotency network through interaction with the core pluripotency-associated transcription factors. Alternatively, GATA6 could mark poised genes that will be induced during lineage-specific differentiation. The 3iL hESCs might therefore provide a tool for understanding the interplay between pluripotency-associated transcription factors and lineage specifiers.

Although we showed that 3iL induces profound transcriptional and epigenetic changes in hESCs, the mechanism for this conversion is not completely understood. Our data demonstrate that 3iL can strongly induce the expression of GP130, which appears to be one of the rate-limiting factors for the activation of LIF signaling in hESCs. It is also conceivable that 3iL, through modulation of cellular signaling, can alter the binding of pluripotency-associated transcription factors by creating new sites. Indeed, we observed that many new or enhanced binding sites occur in 3iL hESCs, and these are significantly associated with a change in expression (Figures 6A–6C). Thus, a rewiring of the regulatory network in response to treatment with 3i and LIF appears to be involved in the cell state conversion.

As genome-scale analyses of regulatory networks require a large number of cells they are generally not feasible for human embryos. However, 3iL hESCs may provide a system for studying gene regulation of pluripotency in the preimplantation blastocyst. Using ChIP-seq profiling of chromatin marks and transcription factor binding sites, we identified many previously

Figure 5. The Epigenomic Landscape of 3iL hESCs

(A) GSEA plots showing enrichment of genes that show increase (red) or decrease (green) of H3K4me3, H3K27ac, and H3K27me3 at promoters in 3iL hESCs compared to hESCs. Genes are ordered by cuffdiff test statistic. Genes that show increased expression in 3iL hESCs are enriched in the set of genes that show increased H3K27ac (Wilcoxon rank-sum test p value = 8.83e-263), increased H3K4me3 (p value = 2.4e-69), and decreased H3K27me3 (p value = 4.90e-92). Genes that show decreased expression in 3iL hESCs are enriched in the set of genes that show decreased H3K27ac (p value < 1.0e-300), decreased H3K4me3 (p value = 3.38e-193), and increased H3K27me3 (p value = 1.44e-12).

(B) Fold change of normalized read counts for histone modifications at promoters of differentially expressed genes, estimated using DESeq2. Genes are ranked by cuffdiff test statistic and normalized per gene.

(C) Fold change of normalized read counts for histone modification at promoters (transcription start sites, TSS) of hESC passage 0-specific genes and epiblast-specific genes. Significance was estimated using the Wilcoxon rank-sum test.

(D) ChIP-Seq profiles of H3K4me3, H3K27ac, and H3K27me3 in 3iL hESCs and hESCs. Pink bars mark regions with increased H3K27ac and/or decreased H3K27me3 in 3iL hESCs. Blue bars mark regions with decreased H3K27ac and/or increased H3K27me3 in 3iL hESCs. Read counts were normalized by the total number of mapped reads.

See also Figure S5.

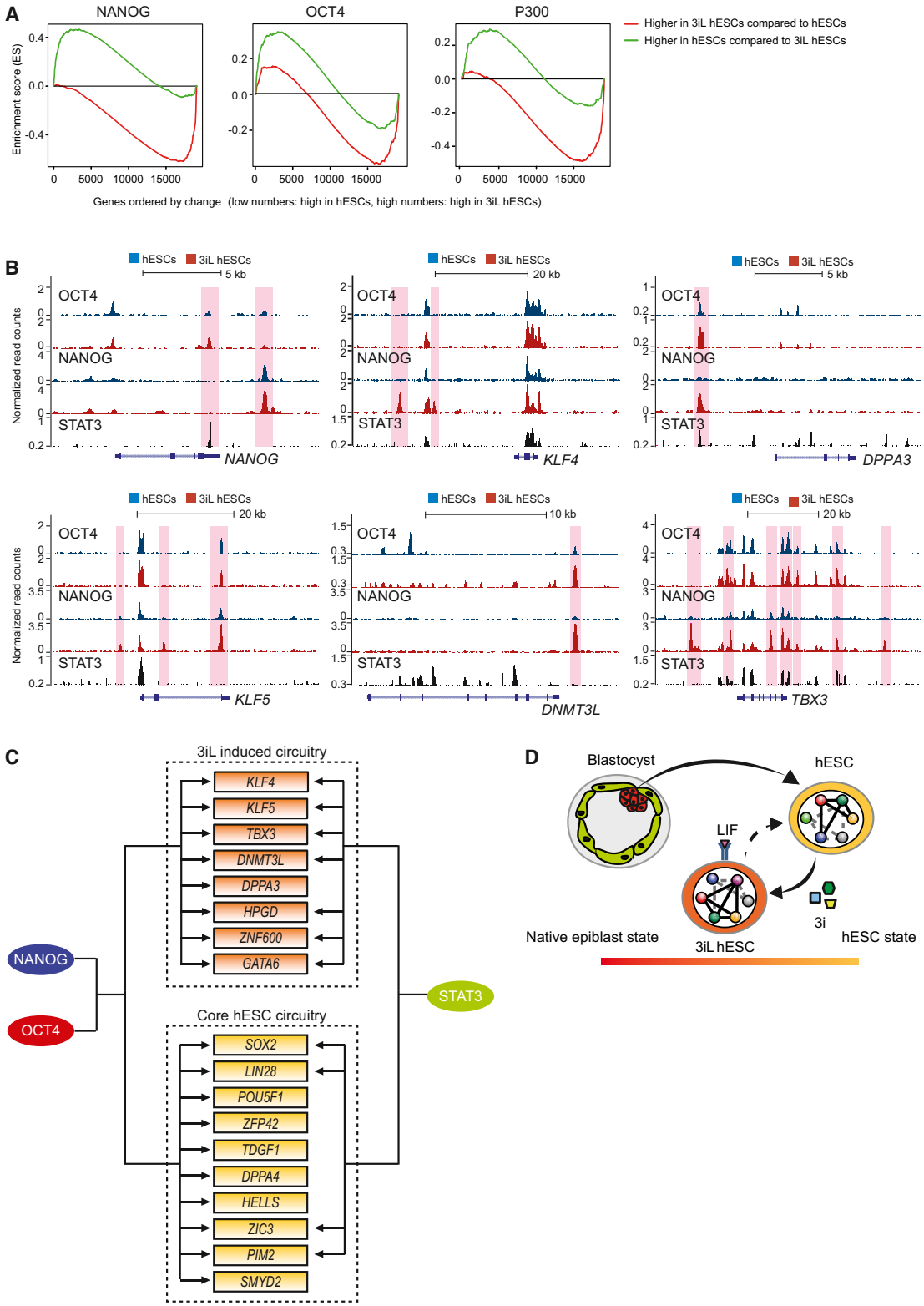

Figure 6. Remodeling of the Pluripotency Transcriptional Network in 3iL hESCs

(A) GSEA plots showing enrichment of genes that show increase (red) or decrease (green) of NANOG, OCT4, or p300 binding nearby. Genes are ordered by cuffdiff test statistic. Genes that show increased expression in 3iL hESCs are enriched in the set of genes that show increased NANOG binding (Wilcoxon rank-sum test p value = 3.97e-38), OCT4 binding (p value = 4.43e-11), and p300 binding (p value = 8.81e-24). Genes that show decreased expression in 3iL hESCs are enriched in the set of genes that show decreased NANOG binding (p value = 7.16e-06) and decreased OCT4 binding (p value = 5.5e-08).

(legend continued on next page)

unknown putative enhancers of genes that are expressed in human preimplantation blastocysts but repressed in hESCs, demonstrating that 3iL hESCs provide insights into functions that have been inaccessible prior to this study. In addition to gene regulation, epigenetic characteristics also differ between 3iL hESCs and hESCs. For example, we observed a global derepression of genes that are expressed in cells from human preimplantation embryos and we find that several epigenetic regulators such as DNMT3L are differentially expressed. DNMT3L regulates DNA methylation, one of the key processes during early embryonic development (Neri et al., 2013). 3iL hESCs may serve as a model system to study these epigenetic pathways and their roles in the regulation of pluripotency.

In conclusion, we report that treatment of hESCs with 3iL induces a pluripotent state that is epigenetically, transcriptionally, and morphologically distinct from conventional hESCs. We demonstrate that a rewired regulatory circuitry in 3iL hESCs supports a native preimplantation epiblast-like expression signature. This more native state of 3iL hESCs presents new opportunities. For example, it will be of great interest to use 3iL culture to reset iPSCs into a more native epiblast-like state, and to explore whether 3iL hESCs can lead to more efficient lineage differentiation. Thus, the study of 3iL hESCs may further revise and extend our understanding of pluripotency of human cells.

EXPERIMENTAL PROCEDURES

Cell Culture

The hESC lines H1 (WA-01, passage 28), hES2 (ES-02, passage 79), and hES3 (ES-03, passage 97) were used for this study. For routine culture of hESCs in TeSR1 (Stem Cell Technologies), cells were cultured feeder free on matrigel (BD). Cell media was changed daily. The hESCs were subcultured with 1 mg/ml Dispase (Stem Cell Technologies) every 5–7 days. 3iL hESCs culture medium contains 1 μM of PD0325901 (Sigma), 2 μM of BIO (Sigma), 2 μM of Dorsomorphin (Sigma), and 10 ng/ml human LIF (Millipore) in TeSR1. 3iL media are prepared fresh and stored at 4°C for not more than 2 weeks. For treatment with 3iL conditions, hESCs cultured in TeSR1 was treated with 3iL 48 hr postseeding. The cells are subsequently subcultured on mitomycin C inactivated mouse fibroblast. Cells are dissociated to single cells using TrypLE (Life Technologies). 3iL medium is refreshed daily and cells are subcultured upon confluency. ROCK inhibitor Thiazovivin is added at a final concentration of 1 μM to enhance cell survival for the first few passages. 3iL hESCs used in all the experiments have been cultured for at least ten passages for adequate conditioning to the new culture condition.

Small-Molecule Compounds Treatment

hESCs were dissociated with dispase and treatment starts 48 hr postseeding. For single chemical and combinatorial chemical treatment, the small molecules are used at the following final concentrations: 0.5 μM A83-01 (Stemgent), 2 μM BIO (Sigma), 3 μM CHIR99021 (Stemgent), 2 μM Dorsomorphin (Sigma), 8 μM Forskolin (Stemgent), 2 μM IDE-1 (Stemgent), 0.5 μM PD153035 (Sigma), 1 μM PD173074 (Sigma), 1 μM PD0325901 (Sigma), 5 μM Pifithrin-α (Sigma), and 1 μM RepSox (Sigma). All small molecules are reconstituted in DMSO. For PI3K pathway inhibition, LY294002 (Sigma) was used at final concentration of 10 μM.

Quantitative PCR and RNA-Seq

For expression analysis, total RNA was extracted using the TRIzol reagent (Invitrogen) and reverse transcribed using the SuperScript II Kit (Invitrogen). Quantitative real-time PCR (qPCR) analysis was performed with the SYBR Green Master Mix (KAPA) using the ABI PRISM 7900 sequence detection system. RNA-Seq libraries were prepared using 4 μg of total RNA according to manufacturer's instructions (TruSeq RNA Sample Preparation Kit v2, Illumina). Samples were multiplexed and sequenced single-read 76 bp (HiSeq 2000, Illumina).

Chromatin Immunoprecipitation

Chromatin immunoprecipitation was performed as previously described (Karwacki-Neisius et al., 2013). ChIP-Seq library was prepared using the NEBNext ChIP-Seq Library kit (NEB Biolabs) according to the manufacturer's instructions and sequenced with the HiSeq 2000 system (Illumina).

Bioinformatics Analysis

RNA-Seq and ChIP-Seq data were mapped against hg19 (Langmead et al., 2009; Trapnell et al., 2009), differential expression was estimated using cuffdiff 2.1.1 (Trapnell et al., 2013). The cuffdiff test statistic was used to rank genes for the gene set enrichment analysis (Subramanian et al., 2005). Single-cell RNA-Seq expression data from preimplantation human embryos were downloaded (Yan et al., 2013), merged with 3iL hESC and hESC RNA-Seq data, and then quantile normalized (Smyth, 2005). Expression values for every gene in every sample were further divided by the sum of the gene's expression. Peak calling was done with MACS (1.4.0) (Zhang et al., 2008). The log-fold change for ChIP-Seq data was calculated using DESeq2 (Anders and Huber, 2010). GSEA plots for ChIP-Seq data were created using the top 1,000 loci with the strongest fold change between 3iL hESCs and hESCs. Box plots were generated in R using standard settings.

ACCESSION NUMBERS

RNA-Seq and ChIP-Seq data are available in the ArrayExpress database (www.ebi.ac.uk/arrayexpress) under accession numbers E-MTAB-2031 (RNA-Seq), E-MTAB-2041(histone modifications), MTAB-2042 (STAT3), and E-MTAB-2044 (OCT4, NANOG, p300, input control).

SUPPLEMENTAL INFORMATION

Supplemental Information includes Supplemental Experimental Procedures, six figures, and five tables and can be found with this article online at http://dx.doi.org/10.1016/j.stem.2013.11.015.

AUTHOR CONTRIBUTIONS

Y.C. designed research, performed experiments, analyzed data, wrote the paper, and supervised the overall project. J.G. performed the bioinformatics

(B) Binding profiles of OCT4, NANOG and STAT3 in 3iL hESCs and hESCs. Pink bars mark regions with increased OCT4 and/or NANOG in 3iL hESCs. Read counts were normalized by the total number of mapped reads.
(C) A rewired transcriptional circuitry in 3iL hESCs. The 3iL induced circuitry (orange boxes) includes genes that are upregulated in 3iL hESCs and are expressed in the native epiblast, among others *TBX3*, *DPPA3*, and *KLF5*. The core pluripotency circuitry network (yellow boxes) consisting of genes such as *POU5F1* and *SOX2* are still part of the new network, highlighting that the 3iL network is rewired, but not replaced. STAT3 also binds to genes of the network (arrows indicated peak with significance score > 150), suggesting that the external signaling network potentially cooperates with the transcriptional network to induce a native epiblast signature in 3iL hESCs.
(D) 3iL supports a LIF-dependent hESC state that more closely resembles the native preimplantation epiblast state. Colored circles represent transcription factors or cell-type-specific factors. Full or dotted lines between circles denote the interactions between these factors in regulating different pluripotent states. The gradient of coloration from red to orange represents the proximity of 3iL hESC and hESC to the pluripotent epiblast cells of human blastocysts.
See also Figure S6 and Tables S2, S3, S4, and S5.

analyses, analyzed the data, and wrote the paper. J.N. performed the experiments, analyzed data, and wrote the paper. X.L., K.G., C.T., W.T., Z.H., and Y.L. performed the experiments. H.N. designed research, analyzed data, wrote the paper, and supervised the overall project.

ACKNOWLEDGMENTS

We are grateful to the Biomedical Research Council (BMRC), Agency for Science, Technology and Research (A*STAR). Jonathan Göke is also supported by a fellowship within the Postdoctoral Programme of the German Academic Exchange Service (DAAD). We acknowledge Valere Cacheux-Rataboul for karyotype analysis and GTB group for sequencing. We would also like to acknowledge the support provided by Paul Robson and the GIS-Fluidigm Single-Cell Omics Center for the single-cell gene expression analysis.

Received: October 23, 2013
Revised: November 4, 2013
Accepted: November 18, 2013
Published: December 5, 2013

REFERENCES

Abe, M., Hasegawa, K., Wada, H., Morimoto, T., Yanazume, T., Kawamura, T., Hirai, M., Furukawa, Y., and Kita, T. (2003). GATA-6 is involved in PPARgamma-mediated activation of differentiated phenotype in human vascular smooth muscle cells. Arterioscler. Thromb. Vasc. Biol. *23*, 404–410.

Anders, S., and Huber, W. (2010). Differential expression analysis for sequence count data. Genome Biol. *11*, R106.

Bao, S., Tang, F., Li, X., Hayashi, K., Gillich, A., Lao, K., and Surani, M.A. (2009). Epigenetic reversion of post-implantation epiblast to pluripotent embryonic stem cells. Nature *461*, 1292–1295.

Boyer, L.A., Lee, T.I., Cole, M.F., Johnstone, S.E., Levine, S.S., Zucker, J.P., Guenther, M.G., Kumar, R.M., Murray, H.L., Jenner, R.G., et al. (2005). Core transcriptional regulatory circuitry in human embryonic stem cells. Cell *122*, 947–956.

Brons, I.G., Smithers, L.E., Trotter, M.W., Rugg-Gunn, P., Sun, B., Chuva de Sousa Lopes, S.M., Howlett, S.K., Clarkson, A., Ahrlund-Richter, L., Pedersen, R.A., and Vallier, L. (2007). Derivation of pluripotent epiblast stem cells from mammalian embryos. Nature *448*, 191–195.

Buecker, C., Chen, H.H., Polo, J.M., Daheron, L., Bu, L., Barakat, T.S., Okwieka, P., Porter, A., Gribnau, J., Hochedlinger, K., and Geijsen, N. (2010). A murine ESC-like state facilitates transgenesis and homologous recombination in human pluripotent stem cells. Cell Stem Cell *6*, 535–546.

Chambers, I., Colby, D., Robertson, M., Nichols, J., Lee, S., Tweedie, S., and Smith, A. (2003). Functional expression cloning of Nanog, a pluripotency sustaining factor in embryonic stem cells. Cell *113*, 643–655.

Chan, E.M., Ratanasirintrawoot, S., Park, I.H., Manos, P.D., Loh, Y.H., Huo, H., Miller, J.D., Hartung, O., Rho, J., Ince, T.A., et al. (2009). Live cell imaging distinguishes bona fide human iPS cells from partially reprogrammed cells. Nat. Biotechnol. *27*, 1033–1037.

Chen, X., Xu, H., Yuan, P., Fang, F., Huss, M., Vega, V.B., Wong, E., Orlov, Y.L., Zhang, W., Jiang, J., et al. (2008). Integration of external signaling pathways with the core transcriptional network in embryonic stem cells. Cell *133*, 1106–1117.

Dahéron, L., Opitz, S.L., Zaehres, H., Lensch, M.W., Andrews, P.W., Itskovitz-Eldor, J., and Daley, G.Q. (2004). LIF/STAT3 signaling fails to maintain self-renewal of human embryonic stem cells. Stem Cells *22*, 770–778.

Do, D.V., Ueda, J., Messerschmidt, D.M., Lorthongpanich, C., Zhou, Y., Feng, B., Guo, G., Lin, P.J., Hossain, M.Z., Zhang, W., et al. (2013). A genetic and developmental pathway from STAT3 to the OCT4-NANOG circuit is essential for maintenance of ICM lineages in vivo. Genes Dev. *27*, 1378–1390.

Dunglison, G.F., Barlow, D.H., and Sargent, I.L. (1996). Leukaemia inhibitory factor significantly enhances the blastocyst formation rates of human embryos cultured in serum-free medium. Hum. Reprod. *11*, 191–196.

Evans, M.J., and Kaufman, M.H. (1981). Establishment in culture of pluripotential cells from mouse embryos. Nature *292*, 154–156.

Furue, M.K., Na, J., Jackson, J.P., Okamoto, T., Jones, M., Baker, D., Hata, R., Moore, H.D., Sato, J.D., and Andrews, P.W. (2008). Heparin promotes the growth of human embryonic stem cells in a defined serum-free medium. Proc. Natl. Acad. Sci. USA *105*, 13409–13414.

Gafni, O., Weinberger, L., Mansour, A.A., Manor, Y.S., Chomsky, E., Ben-Yosef, D., Kalma, Y., Viukov, S., Maza, I., Zviran, A., et al. (2013). Derivation of novel human ground state naive pluripotent stem cells. Nature. Published online October 30, 2013. http://dx.doi.org/10.1038/nature12745.

Göke, J., Chan, Y.-S., Yan, J., Vingron, M., and Ng, H.-H. (2013). Genome-wide kinase-chromatin interactions reveal the regulatory network of ERK signaling in human embryonic stem cells. Mol. Cell *50*, 844–855.

Guo, G., and Smith, A. (2010). A genome-wide screen in EpiSCs identifies Nr5a nuclear receptors as potent inducers of ground state pluripotency. Development *137*, 3185–3192.

Guo, G., Yang, J., Nichols, J., Hall, J.S., Eyres, I., Mansfield, W., and Smith, A. (2009). Klf4 reverts developmentally programmed restriction of ground state pluripotency. Development *136*, 1063–1069.

Guo, G., Huss, M., Tong, G.Q., Wang, C., Li Sun, L., Clarke, N.D., and Robson, P. (2010). Resolution of cell fate decisions revealed by single-cell gene expression analysis from zygote to blastocyst. Dev. Cell *18*, 675–685.

Hanna, J., Cheng, A.W., Saha, K., Kim, J., Lengner, C.J., Soldner, F., Cassady, J.P., Muffat, J., Carey, B.W., and Jaenisch, R. (2010). Human embryonic stem cells with biological and epigenetic characteristics similar to those of mouse ESCs. Proc. Natl. Acad. Sci. USA *107*, 9222–9227.

Humphrey, R.K., Beattie, G.M., Lopez, A.D., Bucay, N., King, C.C., Firpo, M.T., Rose-John, S., and Hayek, A. (2004). Maintenance of pluripotency in human embryonic stem cells is STAT3 independent. Stem Cells *22*, 522–530.

Ip, N.Y., Nye, S.H., Boulton, T.G., Davis, S., Taga, T., Li, Y., Birren, S.J., Yasukawa, K., Kishimoto, T., Anderson, D.J., et al. (1992). CNTF and LIF act on neuronal cells via shared signaling pathways that involve the IL-6 signal transducing receptor component gp130. Cell *69*, 1121–1132.

Karwacki-Neisius, V., Göke, J., Osorno, R., Halbritter, F., Ng, J.H., Weiße, A.Y., Wong, F.C., Gagliardi, A., Mullin, N.P., Festuccia, N., et al. (2013). Reduced Oct4 expression directs a robust pluripotent state with distinct signaling activity and increased enhancer occupancy by Oct4 and Nanog. Cell Stem Cell *12*, 531–545.

Kimber, S.J., Sneddon, S.F., Bloor, D.J., El-Bareg, A.M., Hawkhead, J.A., Metcalfe, A.D., Houghton, F.D., Leese, H.J., Rutherford, A., Lieberman, B.A., and Brison, D.R. (2008). Expression of genes involved in early cell fate decisions in human embryos and their regulation by growth factors. Reproduction *135*, 635–647.

Kuijk, E.W., van Tol, L.T., Van de Velde, H., Wubbolts, R., Welling, M., Geijsen, N., and Roelen, B.A. (2012). The roles of FGF and MAP kinase signaling in the segregation of the epiblast and hypoblast cell lineages in bovine and human embryos. Development *139*, 871–882.

Langmead, B., Trapnell, C., Pop, M., and Salzberg, S.L. (2009). Ultrafast and memory-efficient alignment of short DNA sequences to the human genome. Genome Biol. *10*, R25.

Li, W., Wei, W., Zhu, S., Zhu, J., Shi, Y., Lin, T., Hao, E., Hayek, A., Deng, H., and Ding, S. (2009). Generation of rat and human induced pluripotent stem cells by combining genetic reprogramming and chemical inhibitors. Cell Stem Cell *4*, 16–19.

Li, W., Li, K., Wei, W., and Ding, S. (2013). Chemical approaches to stem cell biology and therapeutics. Cell Stem Cell *13*, 270–283.

Lu, J., Hou, R., Booth, C.J., Yang, S.H., and Snyder, M. (2006). Defined culture conditions of human embryonic stem cells. Proc. Natl. Acad. Sci. USA *103*, 5688–5693.

Ludwig, T.E., Levenstein, M.E., Jones, J.M., Berggren, W.T., Mitchen, E.R., Frane, J.L., Crandall, L.J., Daigh, C.A., Conard, K.R., Piekarczyk, M.S., et al. (2006). Derivation of human embryonic stem cells in defined conditions. Nat. Biotechnol. *24*, 185–187.

Martin, G.R. (1981). Isolation of a pluripotent cell line from early mouse embryos cultured in medium conditioned by teratocarcinoma stem cells. Proc. Natl. Acad. Sci. USA *78*, 7634–7638.

Montserrat, N., Nivet, E., Sancho-Martinez, I., Hishida, T., Kumar, S., Miquel, L., Cortina, C., Hishida, Y., Xia, Y., Esteban, C.R., and Izpisua Belmonte, J.C. (2013). Reprogramming of human fibroblasts to pluripotency with lineage specifiers. Cell Stem Cell *13*, 341–350.

Neri, F., Krepelova, A., Incarnato, D., Maldotti, M., Parlato, C., Galvagni, F., Matarese, F., Stunnenberg, H.G., and Oliviero, S. (2013). Dnmt3L antagonizes DNA methylation at bivalent promoters and favors DNA methylation at gene bodies in ESCs. Cell *155*, 121–134.

Nichols, J., and Smith, A. (2012). Pluripotency in the embryo and in culture. Cold Spring Harb. Perspect. Biol. *4*, a008128.

Niwa, H., Burdon, T., Chambers, I., and Smith, A. (1998). Self-renewal of pluripotent embryonic stem cells is mediated via activation of STAT3. Genes Dev. *12*, 2048–2060.

Plusa, B., Piliszek, A., Frankenberg, S., Artus, J., and Hadjantonakis, A.K. (2008). Distinct sequential cell behaviours direct primitive endoderm formation in the mouse blastocyst. Development *135*, 3081–3091.

Reijo Pera, R.A., DeJonge, C., Bossert, N., Yao, M., Hwa Yang, J.Y., Asadi, N.B., Wong, W., Wong, C., and Firpo, M.T. (2009). Gene expression profiles of human inner cell mass cells and embryonic stem cells. Differentiation *78*, 18–23.

Roode, M., Blair, K., Snell, P., Elder, K., Marchant, S., Smith, A., and Nichols, J. (2012). Human hypoblast formation is not dependent on FGF signalling. Dev. Biol. *361*, 358–363.

Shu, J., Wu, C., Wu, Y., Li, Z., Shao, S., Zhao, W., Tang, X., Yang, H., Shen, L., Zuo, X., et al. (2013). Induction of pluripotency in mouse somatic cells with lineage specifiers. Cell *153*, 963–975.

Silva, J., Nichols, J., Theunissen, T.W., Guo, G., van Oosten, A.L., Barrandon, O., Wray, J., Yamanaka, S., Chambers, I., and Smith, A. (2009). Nanog is the gateway to the pluripotent ground state. Cell *138*, 722–737.

Singh, A.M., Reynolds, D., Cliff, T., Ohtsuka, S., Mattheyses, A.L., Sun, Y., Menendez, L., Kulik, M., and Dalton, S. (2012). Signaling network crosstalk in human pluripotent cells: a Smad2/3-regulated switch that controls the balance between self-renewal and differentiation. Cell Stem Cell *10*, 312–326.

Smyth, G.K. (2005). limma: Linear Models for Microarray Data. In Bioinformatics and Computational Biology Solutions Using R and Bioconductor, R. Gentleman, V. Carey, W. Huber, R. Irizarry, and S. Dudoit, eds. (New York: Springer), pp. 397–420.

Subramanian, A., Tamayo, P., Mootha, V.K., Mukherjee, S., Ebert, B.L., Gillette, M.A., Paulovich, A., Pomeroy, S.L., Golub, T.R., Lander, E.S., and Mesirov, J.P. (2005). Gene set enrichment analysis: a knowledge-based approach for interpreting genome-wide expression profiles. Proc. Natl. Acad. Sci. USA *102*, 15545–15550.

Tesar, P.J., Chenoweth, J.G., Brook, F.A., Davies, T.J., Evans, E.P., Mack, D.L., Gardner, R.L., and McKay, R.D. (2007). New cell lines from mouse epiblast share defining features with human embryonic stem cells. Nature *448*, 196–199.

Thomson, J.A., Itskovitz-Eldor, J., Shapiro, S.S., Waknitz, M.A., Swiergiel, J.J., Marshall, V.S., and Jones, J.M. (1998). Embryonic stem cell lines derived from human blastocysts. Science *282*, 1145–1147.

Trapnell, C., Pachter, L., and Salzberg, S.L. (2009). TopHat: discovering splice junctions with RNA-Seq. Bioinformatics *25*, 1105–1111.

Trapnell, C., Hendrickson, D.G., Sauvageau, M., Goff, L., Rinn, J.L., and Pachter, L. (2013). Differential analysis of gene regulation at transcript resolution with RNA-seq. Nat. Biotechnol. *31*, 46–53.

Vallier, L., Alexander, M., and Pedersen, R.A. (2005). Activin/Nodal and FGF pathways cooperate to maintain pluripotency of human embryonic stem cells. J. Cell Sci. *118*, 4495–4509.

Vassena, R., Boué, S., González-Roca, E., Aran, B., Auer, H., Veiga, A., and Izpisua Belmonte, J.C. (2011). Waves of early transcriptional activation and pluripotency program initiation during human preimplantation development. Development *138*, 3699–3709.

Wang, W., Yang, J., Liu, H., Lu, D., Chen, X., Zenonos, Z., Campos, L.S., Rad, R., Guo, G., Zhang, S., et al. (2011). Rapid and efficient reprogramming of somatic cells to induced pluripotent stem cells by retinoic acid receptor gamma and liver receptor homolog 1. Proc. Natl. Acad. Sci. USA *108*, 18283–18288.

Yan, L., Yang, M., Guo, H., Yang, L., Wu, J., Li, R., Liu, P., Lian, Y., Zheng, X., Yan, J., et al. (2013). Single-cell RNA-Seq profiling of human preimplantation embryos and embryonic stem cells. Nat. Struct. Mol. Biol. *20*, 1131–1139.

Yang, J., van Oosten, A.L., Theunissen, T.W., Guo, G., Silva, J.C., and Smith, A. (2010). Stat3 activation is limiting for reprogramming to ground state pluripotency. Cell Stem Cell *7*, 319–328.

Yao, S., Chen, S., Clark, J., Hao, E., Beattie, G.M., Hayek, A., and Ding, S. (2006). Long-term self-renewal and directed differentiation of human embryonic stem cells in chemically defined conditions. Proc. Natl. Acad. Sci. USA *103*, 6907–6912.

Zhang, Y., Liu, T., Meyer, C.A., Eeckhoute, J., Johnson, D.S., Bernstein, B.E., Nusbaum, C., Myers, R.M., Brown, M., Li, W., and Liu, X.S. (2008). Model-based analysis of ChIP-Seq (MACS). Genome Biol. *9*, R137.

Zhang, Y., Li, W., Laurent, T., and Ding, S. (2012). Small molecules, big roles — the chemical manipulation of stem cell fate and somatic cell reprogramming. J. Cell Sci. *125*, 5609–5620.

Zhou, H., Li, W., Zhu, S., Joo, J.Y., Do, J.T., Xiong, W., Kim, J.B., Zhang, K., Schöler, H.R., and Ding, S. (2010). Conversion of mouse epiblast stem cells to an earlier pluripotency state by small molecules. J. Biol. Chem. *285*, 29676–29680.